Proc. Ind. Assoc. Cult. Sci. **80B** (5), p1–p29 (1997)

IJP E
an international journal

Raman scattering, photo-luminescence and their correlation with micro-nano-structures*

H D Bist

Emeritus Scientist (CSIR), Department of Physics, Indian Institute of Technology, Kanpur, Kanpur-208 016, India

Manuscript Received on 25 July, 1997

Abstract : Experimental requirements for a modern laser Raman scattering (RS) [and photo-luminescence (PL)] laboratory have been reviewed. It is demonstrated that RS and PL studies can be used to peep into the micro-nano-structures of materials.

Keywords : Raman scattering, photo-luminescence, Cd–Te, GaAs/$Al_xGa_{1-x}As$ oval defects

PACS Nos. : 33.20 Fb, 78.55.–m, 81

1. Introduction

It is indeed a pleasure and priviledge for me to be invited to Indian Association for the Cultivation of Science to deliver the 7th S C Sirkar Memorial Lecture today. These lectures, I was told, have been delivered earlier by noted physicists Drs. S S Jha, G S Agarwal, (late) P S Narayanan, D K Rai, D D Pant, *etc.* I express my hearty thanks to Professor D Chakravorty, Director of IACS, Professor S K Mukherjee, the President of the IACS and Professor T N Misra, Head Spectroscopy Department, for giving me this great honour of visiting your august and ranking Institution at Calcutta. Bengal represents the Indian Science and Culture since the educational renaissance in the country. All international honours in science, literature and humanities to India (through 4 nobel laureates like

*VII S C Sirkar Memorial Lecture—1996 delivered at the Indian Association for the Cultivation of Science, Jadavpur, Calcutta-700 032, India on December 20, 1996

Sri Ravindra Nath Tagore, Sir C V Raman, Dr S Chandrasekhar, Mother Teresa and others like Dr S N Bose, Dr M N Saha and J C Bose *etc.*) have to be associated with Calcutta (Bengal). The Indian religious outlook was propagagted by persons like Sri Aurbindo and Swami Vivekanand. Philanthropist like Mohendralal Sircar and vice-chancellors like Sir Ashutosh Mukherjee laid the foundation for cultivating and promoting geniuses like Sir C V Raman at this place. In the words of Sir C V Raman in his lecture on 4th July, 1931 on the occasion of civic reception to him by the Calcutta Corporation "Calcutta has been the intellectual metropolis not only of Bengal, or of India, but of the whole of Asia from which has gone forth a living stream of knowledge in many branches of study". In the same year in a message to the citizens of Calcutta, Raman remarked "the opportunities that have come to me to serve the cause of science and our country is due to the efforts of Calcutta's two greatest citizens in the past–Dr Mohendralal Sircar and Sir Ashutosh Mukherjee. To them and to many others, happily still living, I owe a deep debt. May I express my gratitude" I reemphasize the above remarks of Sir C V Raman to present living and past functionaries of this Institute on my behalf for their efforts in advancing science and technology

It is my understanding that these (annual lectures) are dedicated to the memory of Dr Sukumar Chandra Sirkar, who was a student, a research assistant, a lecturer, a Professor and Head, an acting Director, Emeritus Professor and President at IACS. His leadership was responsible for the creation of three independent departments in physics (X-ray and magnetism, optics, and theoretical physics at this Institute The efforts of people like him and Professor Raman should be additional inspiration for the scientists in IACS, Calcutta. Very good work is being done in spectroscopy today at this Institute by Professors Mihir Chowdhury, T N Misra and others in the relevant departments. As one of the contemporary workers in the field, I have tried to make a small contribution in the Indian scientific scenario in the Raman field. I was able to establish a modern Laser Raman Laboratory and guide average number of PhD, MSc (Theses) students at IIT, Kanpur. I have touched many areas of molecular and solid state spectroscopy. However, the more lasting successful efforts I consider the organization of three international (national) conferences and publication of their proceedings in the form of four books. Even more important than this has been bringing out of the two books in the form of status reports in India with a world overview and useful information in Indian Laser and cognate fields. Out of the six books given at the end of this lecture [1–6], I would like to present my two recently co-edited and co-authored books to Prof D Chakravorty, as a mark of my current visit to this Institute.

These S C Sirkar Memorial lectures are also dedicated to the persuit of science in India. I have chosen the topic 'Raman Scattering (RS), Photoluminescence (PL) and their Correlation with Micro-, Nano-Structures' today. The title reflects immediately, how experiments on RS and PL can be correlated with modern experimental results from micro-nano structural determinations.

2. Characterization of materials

More than fifty techniques for physicochemical characterization are being used to probe various aspects of materials [7]. Mechanical methods are used to determine the elastic constants, Young's modulus *etc*. Thermal characterization methods extensively used are those based on measurements of thermal expansion, specific heat, heat capacity, differential thermal analysis, scanning calorimetry, thermoelectric power *etc*. Electrical properties (like resistivity, Hall coefficient, dielectric constant, permittivity); magnetic-susceptibility, -anisotropy and resonance [electron paramagnetic, nuclear and quadrupole *etc*] methods have been used for material characterization. For structural determinations, the techniques of X-ray, neutron-, electron-diffraction, scanning electron microscopy, scanning tunneling microscopy, scanning atomic force microscopy *etc* have become very common.

The optical absorption and emission (in ultraviolet, visible and infrared regions), and the scattering (neutron inelastic, Raman and Brillouin) methods have been used extensively to characterize the composition, and structure of materials [7]. Raman spectroscopy has evolved as a powerful, non-destructive, non-contact analytical tool with well-established credentials for molecular (and bond) specificity. Simultaneous developments in the field of lasers and other essential techniques gave a tremendous boost to Raman spectroscopy In this paper our recent micro Raman and PL work on the thin films of GaAs/Al_xGa_{1-x} As, and CdTe are being presented, along with a review of Raman experimental requirements.

3. Lasers

Since the first discovery of laser action in Ruby by Maiman in 1960, the world has witnessed an immense growth of activity in laser area; both in its fundamental and applied aspects At present lasers are available, some with commercial and many with individual scientific organizations, spanning the electromagnetic spectrum from sub-millimeter waves to soft X-rays; their output power varies anywhere between a few micro watts to a million billion watts. Lasers have been developed which can be operated in either CW or in pulsed mode with extremely short durations like a few femtoseconds. Ultra high resolution, single frequency lasers, with bandwidth of a few Hz have also been developed. Wide use of lasers is due to the specific properties of laser radiation. The laser is a generator of coherent light. The temporal coherence of lasers has resulted in phenomenal enhancement in monochromaticity and spectral energy density; and the spatial coherence has resulted in extremely high directionality. Consequently a very high intensity per steradian and correspondingly high areal energy density at the diffraction limited focussed spot (as small as wavelength) is obtained. In Table 1 we list some capsuled information about the different kinds of lasers in use. The column on the year of commercial production of each laser is of some interest. The Nd : YAG and He-Ne laser came into commercial production within one and two years, respectively after they were discovered. A laser like the copper vapor laser had to await 15 years for its commercial production. Iodine photo-dissociation lasers commercialized, 19 years after their discovery. Table 1 also gives an indication of the major areas of the applications of the different lasers. Laser development in the future will be

along one or more of the following lines : (i) New wavelengths : towards higher energy side (vacuum UV, soft X-ray) and very low energy (far infrared) side. (ii) Shorter pulses : pico, femto, sub-femto seconds. (iii) High powers : CW ; pulse peak, high efficiency.

Table 1. Capsuled information about the history of different lasers and their areas of applications. The superscript 1, 2, 3 in the table show :

1 : the year of discovery of laser, while its year of commercialization is given in parentheses 2 : CW = continuous wave output, HC = high coherence, figure within parentheses gives output power, HEP = high energy pulse, HPP = high power pulse, QSC = Q switching capability 10–20% efficiency 3 : A = alignment, measurement and control, BP = basic processes, study of, C = communications, CRP = chemical reaction processing, D = display and entertainment, DLP = dye laser, F = lightsource of facsimile, GA = graphic arts, H = holography, HSH = high speed holography, IP = information processing, IR = infrared region, L = lithography, LR = laser radar, MD = medical diagnosis, MP = material processing, MR = materials research, MT = medical treatment, NF = nuclear fusion, PG = plasma generation, RS = remote sensing, RSS = Raman scattering source, S = spectroscopy, SI = simulation (military), VD = video disk, WD = weapons development

Lasers	Prominent wavelength (μm)	Year[1]	Special features[2]	Applications[3]
Gas Lasers				
CO_2	10.6	1964	IR, η = 10–20%, CW	BP, C, MP, MT
		(1966)	(1 W–1 kW), HEP	NF, PG, RS, S, WD
Chemical . HF, DF	2.6–4	1967		BP, S, WD
		(1977)		
Excimer				
ArF, KrCl	193, 0.222,	1975		BP, CRP, B, MP
KrF, XeBr	0.248, 0.282	(1976)		MT, S, WD, RSS
XeCl, XeF	0 308, 0.351			
Laser pumped	20–1000	1963		BP, S
Direct discharge		(1969)		
He–Ne	0.633	1960	CW (0.1–50 mW)	A, C, D, F, GA
		(1962)	HC	IP, S, VD, RSS
I_2 Photo-dissociation	1.315	1964		BP, MP, S
Ion lasers				
Ar^+	0.488, 0.5145	1964	CW (1–10 W), HC	A, BP, D, GA, H, IP
		(1966)		MD, MP, MT, RSS
Kr^+	0.647, 0.530			
Metal vapour				
Cu vapour	0.510, 0.578	1966		BP, MP, S
		(1981)		
He-Cd	0.442, 0.325	1968	UV (CW)	A, GA, H, IP, MD
		(1970)	(1–50 mW)	MR, RS, S
An Vapour	0.628	1978		MT
		(1982)		
N_2	0.337	1966		BP, S
		(1969)		

Table 1. *(cont'd.).*

Lasers	Prominent wavelength (μm)	Year[1]	Special features[2]	Applications[3]
Liquid Dye Lasers				
CW dye	0 400–1.0	1970 (1971)		BP, MT, S
Pulsed dye	0 320–0.970	1966 (1969)		BP, MT, S
Solid (insulator)				
Nd Glass	1 06	1961 (1968)	HEP (1000 J) HPP (TW)	BP, MP, WD, PG
Nd YAG	1.06	1964 (1965)	HEP, CW (1 W–1 kW), HPP, SHG 100 kW (5 kHz)	BP, D, DLP, GA MP, MT, AS, RSS S, DLP, LR
Ruby	0 694	1960 (1963)	HEP (0 1 to 100 J) HPP (1 mW to 10 GW) QSC	A, HSH, MP RRF, S
Color centre	1 5–3 3	1965 (1977)		BP, S
Alexandrite	0 700–0 815	1977 (1981)		MP
Solid (semiconductor)				
Single frequency diode		1962 (1965)		
GaAs	0 904			A, F, GA, IP, SI, VD
GaAlAs	0 8–0.9			A, C, GA, IP
InGaAsP	1.3–1.6			C
Tunable diode (lead salt)	2–30	1964 (1975)		A, S

(iv) Compactness, small dimensions; light weight; lower cost; higher life; ruggedness may make semiconductor lasers as the first choices for the 21st century devices. However, simultaneous work will be needed in high-speed electronics, precision optical hardware and associated devices.

3 1. Lasers in Raman, stimulated-Raman, nonlinear optics and spectroscopy:

The development and production of lasers of a vast variety have created a tremendous impact in the field of Raman Spectroscopy. In fact, the difficult period of the Raman field ended around 1964; and a renaissance started with the application of reliable lasers as excitation sources. Typical characterisation of Ar^+, Kr^+ and He-Ne laser lines are given in Table 2 In several areas there has been a major change in the data acquisition capabilities on account of the larger flux densities available from lasers. In other areas the high monochromaticity of lasers has advanced precision. Likewise, tunability has added to the

depth and convenience of study of the energy levels. Deeply coloured or even black or highly fluorescent materials, high temperature gases flames could be handled for Raman work.

Table 2. Lasing lines of most frequent Ar and Kr ion lasers

	Air-wavelength (nm)	Air wavenumber	Power (mW)
Ar[a]	457 9 (violet)	21838.8	300
	465 8	21468 4	130
	472 7	21155 1	250
	476 5 (blue)	20986.4	600
	488.0 (blue)	20491 8	1300
	496 5	20141.0	600
	501 7 (green)	19932 2	300
	514 5 (green)	19436 3	1700
	528.7 (yellow-green)	18914 3	300
Kr[b]	476 2	20999 6	60
	482.5	20725 4	45
	520 8	19201 2	90
	530 9	18835 9	200
	568 2	17599.4	200
	647 1 (red)	15453 6	500
	676 4	14784 2	120
	752 5	13289 0	100
	799 3	12510 9	30
Ne[c]	632 8 (red)	15802.8	50

Spectra-Physics Models [a] 164–08, [b] 164 01 and [c] 125 A.

With the advent of lasers new areas of research, hitherto inconceivable, have emerged both in fundamental and applied sciences. High resolution and non-linear spectroscopy; time and frequency domain spectroscopy of atoms and molecules; non-linear optics with solids and liquids, and applications in varied fields from all types of structural applications and finger print type identification for materials from deep under the earth and oceans, in fire and flames, in the sky upto astronomical distances and in air have become possible.

The field of non-linear optics and spectroscopy is now 35 years old, if one associates its birth with the observation of second harmonic generation by Franken *et al.* in 1961. In any non-linear process conservation of momentum and energy has to be satisfied and the resultant wave is determined by the special features of both the combining waves and the medium. The Raman related stimulated (coherent) processes that could be studied theoretically and observed experimentally are those of (i) stimulated Brillouin-, stimulated Rayleigh- and Rayleigh-wing-, and stimulated Raman scattering. Hyper-Rayleigh and hyper

Raman scattering, coherent-anti-Stokes Raman scattering (CARS), continuous resonance CARS, Coherent Stokes Raman Scattering (CSRS), Inverse Raman Scattering (IRS), Stimulated Raman gain spectroscopy (SRGS), photoacoustic Raman spectroscopy (PARS), Raman induced Kerr-effect spectroscopy (RIKES), asterisk spectroscopy and higher order Raman excitation studies (HORSES), all fall under stimulated coherent processes. The new lasers at desired wavelengths have been realized at several laboratories practically. Photoluminescence (PL) is an old phenomena of emission by one photon process and could be studied easily by a Raman set up as the quantum efficiency of PL could be upto unity while that of rudimentary Raman scattering is of the order of 10^{-6} to 10^{-8}. The other new area has its origin in the production of laser pulses of extremely short duration. Its consequence is time-resolved Raman spectroscopy, which has opened up a vast scope for the study of fast transient phenomena; relaxation processes, short-lived species, and so on and so forth

4. Sample handling and illumination

It is worth mentioning that sample handling techniques vary with the nature and type of the materials to be investigated. The hygroscopic, dehydrating or air-sensitive (especially to oxygen or water in air) or corrosive (toxic) materials can be studied by sealing them under proper environmental conditions in a pyrex (non-fluorescent) glass or quartz container. Low pressure gases need to be sealed (epoxied by non-fluorescent cement) inside cells with Brewster angle quartz windows (for use of multiple reflection technique) and also need high power lasers for excitation.

Microcrystalline or powder materials could be enclosed in capillary tubes or any other suitably shaped vessels. Pellet techniques are used for small amounts (50 mg) of sample to press after sprinkling it on the KBr pellet while still on a die. Local heating of sample could be reduced by diluting the (absorbing) materials in a matrix.

Rotating techniques for liquid and solid samples are available commercially to avoid heating (and hence decomposition, phase change *etc* of the samples, especially if they have absorption at the excitation wavelength. Defocussing the laser beam or using a cylindrical lens for focussing the laser beam to give image of 10 to 25 mm length instead of few microns on to the sample also reduces this problem by reducing the power density per unit area by a factor of about 10^3.

4.1. Common excitation-collection geometries :

The common excitation collection geometries use a 90° collection of scattered radiation for Raman and photoluminescence studies, as the strong Rayleigh line and Rayleigh wing scattering will interfere strongly in other geometries with the feeble rudimentary Raman scattering. The variations of 90° geometries using a simple lens, an achromatic combination of lenses, and an elliptical mirror-plane mirror combination in which the samples and the entrance slit of the spectrometer are located on two focii of the ellipse are shown in

Figure 1(a), (b) and (c), in that order. Figure 1(d) shows a back-scattering, 180° collection, geometry used under specific experimental conditions; *e.g.* for highly absorbing materials,

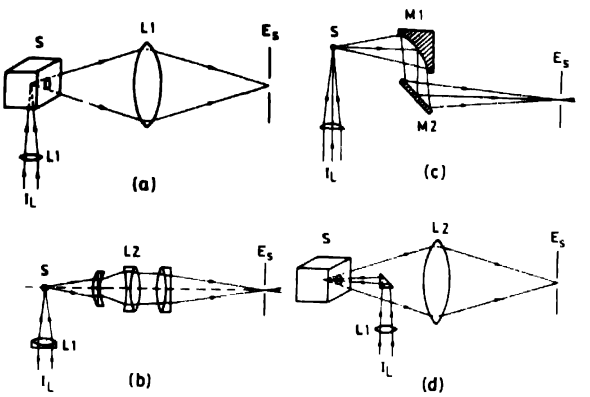

Figure 1. The common Raman (and PL) excitation-collection geometries . (a), (b), (c) are variation in 90° collection and (d) represents 180° collection geometry I_L = incident laser beam, L_1 focussing lens, S = sample, L_2 = collecting lens (or achromatic lens combination, M_1 = elliptical and M_2 plane mirror, P = prism and E_s = entrance slit of the spectrophotometer

or where equipment needs it *e.g.* with microscope (Micro-Raman) instruments, and other special techniques (low, temperature studies) single crystals with one face polished situations *etc.*

4.2. Gases :

The developments that have taken place in the field of Raman spectroscopy during almost seven decades could be divided into three distinct phases. During the first two decades

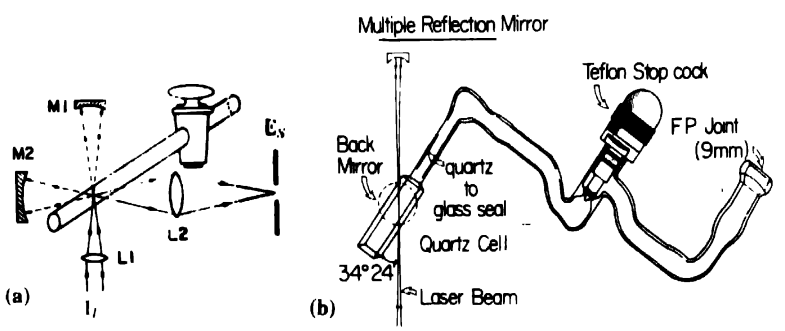

Figure 2. Raman (and PL) studies with gases using : (a) ordinary cylindrical cell (variation of it with 1 cm diameter, ≈6 cm length fitted with quartz windows at fixed Brewster angle is commercially available) (b) 1 × 1 × 3 5 cm cell with quartz-glass graded seal and teflon stopcock with viton rings

primarily the liquids and solids were studied with few exception; *e.g.* few gases using Rasetti technique [8]. Around 1947, the water cooled low pressure mercury arc lamps with

high currents (Toronto arc) were developed [9,10]. Using the multiple reflection mirror system and good Raman spectrophotometers, Raman study of gases also became possible. With the invention of lasers after 1960 tremendous revival of interest in the overall field of Raman spectroscopy occurred as has already been mentioned. For gaseous systems use of multiple reflection cell, especially at low pressures, is essential. Two of the common geometries, using a capillary and a 1 cm quartz cell, an order of magnitude change in Raman intensity by using multiple reflection, and almost doubling the collected scattered intensity by use of back-reflecting mirror of proper focal length, are given in Figure 2(a) and 2(b), the latter being envisaged by the author where the tilt of the cell could be adjusted

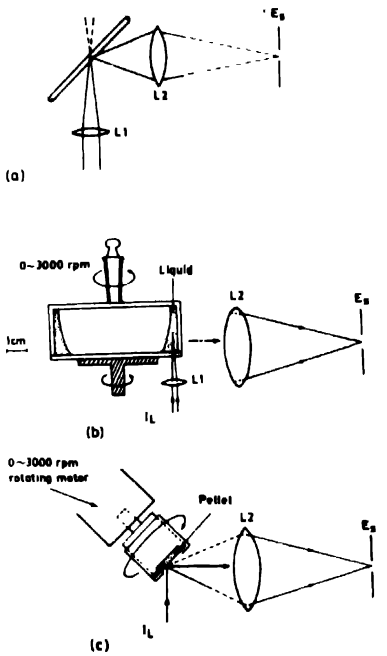

Figure 3. Raman (and PL) study in condensed phase . (a) transparent samples using a capillary tube of quartz and absorbing samples using a rotating cell, (b) liquids, (c) solids

with variations of, even the refractive index of the cell material (quartz, glass) or gases inside it to get maximum intensity [11]. The use of teflon stopcock eliminates sample contamination with interaction of corrosive gases with the grease of normal stopcocks. The multiple reflection arrangement, allows to use lower pressure and avoid complications due to reabsorption by the sample, the thermal lens effect and thermal/photo-decomposition of the sample due to excessive heat.

The cell has also been used for the study of ordinary Raman effect, resonant Raman scattering and resonance fluorescence studies from gases, solutions and neat liquids under abnormal conditions [11]. While working with gases, the possibility of sudden explosion due to higher pressure (due to reaction, decomposition *etc*) should be avoided by using about 2 to 3 mm thick, 15 mm outer diameter quartz tube [12].

4.3. Condensed phase :

The three common cells used for Raman and photoluminescence studies of (a) transparent (b) absorbing liquid and (c) solids are represented in Figure 3. The capillary technique could be used for any liquid or solid. The rotating cell (or laser beam) gives a relative motion between the exposed portion of liquid or solid and the incident laser radiation. This technique avoids excessive heating and consequent thermal effects. The principle of rotating cell was patented by Kiefer and Bernstein [13].

4.4. Specialized techniques .

With the application of fiber optics in the Raman field, the conditions under which Raman spectra could be obtained are limited only by the ingenuity of the scientist for the particular problem. A few of the techniques could be mentioned below :

(i) Micro (nano) sized samples

Using microscope objectives for illumination (and collection) of diffraction limited spots, commercial micromate (Spex-Industries) and MOLE (Jobin Yvon) *etc* could distinguish spectra spatially upto about one micron on the sample. The primary problem with micro-Raman technique is local heating due to extremely high power density at the focussed spot. Using specialized subtraction techniques by manipulating the irradiation spot, one could get information upto nano (pico-) sized regions, especially using cylindrical focussing [14].

4.5. Low and high temperature studies :

Various types of special devices are made to keep the samples at specified controlled temperatures. The low temperature cell, fabricated and used in our laboratory is shown in Figure 4(a). A double walled pyrex glass structure has an inner jacket at the bottom of which is attached through a kovar seal a rectangular copper attachment (cold finger) for holding the sample. The outer jacket has two quartz windows, one each for the incident laser beam and for collection of the scattered radiation, respectively. Liquid nitrogen is used as the coolant for the copper block (and the sample in it). To obtain temperature upto 63 K an arrangement was made to evaporate the liquid nitrogen under reduced pressure using high capacity rotary pumps. A 25-watt heater attached to the sample holder was used to control the temperature (within ± 2 K; and a Cu–Co thermocouple to measure the sample temperature within ± 1 K. Special sealing material, resistant to low temperatures, is to be used for work below liquid nitrogen temperature.

A variable temperature cell to obtain spectra upto liquid nitrogen temperature is that designed by Miller and Harney [15] and shown in Figure 4(b). The sample is kept inside a thin walled melting point tube, which is placed at the center of an evacuated annular jacket, and cold nitrogen gas is passed through the center of the jacket. Any temperature down to −150°C can be achieved easily [16]. The temperature is measured with a thermocouple placed near the sample. This device is also used for obtaining Raman spectra at high temperatures by using hot air instead of cold nitrogen.

The spectra above 300 K upto (≈ 600 K) were recorded with a locally fabricated cell (figure 5a). It consists of three parts : (i) the sample holder(s), (ii) the heating block, and (iii) the temperature controller.

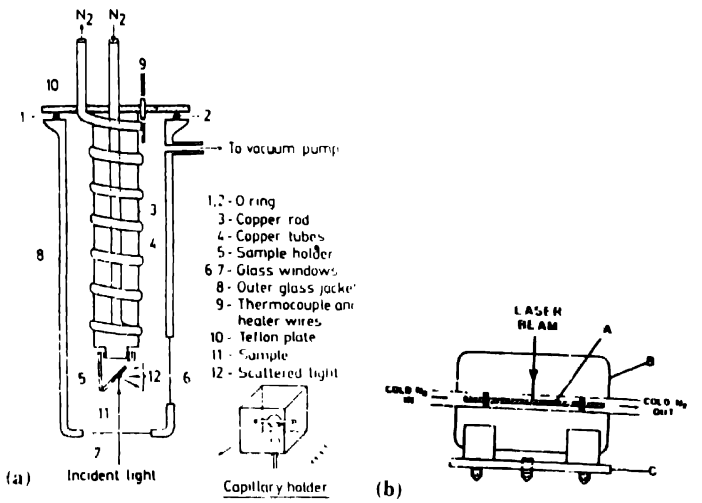

Figure 4. Design of low temperature cell for Raman (and PL) studies in the range 63 to 300 K (a) components as marked, (b) Harney-Miller type A sample tube, B, evacuated annular jacket for insulation, C metal support

The brass heating block 18 × 18 × 38 mm^3 has an 8 mm diameter hole drilled to a depth of 28 mm to insert the sample holder. The block is heated from three sides by 25 watt heaters fitted into grooves. On the bottom and on the fourth side two conical holes are drilled for the incident laser beam and for the collection of scattered radiations, respectively. The system is mounted on a Spex three-way motion platform for alignment of the sample. Sample holders to study temperature dependence of liquids, polycrystalline and single crystal samples have been improvised in the lab (Figure 5). One Cu-Co thermocouple is used to measure the temperature and another thermocouple for its control through a relay upto 600 ± 1 K. Figure 5(b) gives the details of another high temperature windowless Pt 10% Rh wire wound for heating the sample upto 1400 K at ambient pressures [17]

4.6 High pressure spectroscopy :

High pressure Raman spectra often provide valuable information about intermolecular interactions; vibrational assignments and thermodynamic properties at high pressure, structural and bonding changes; phase transitions driven by soft modes; *etc.* Raman measurements can be used to complement direct structural determination from X-ray, neutron diffraction experiments, scanning electron microscopy (SEM), transmission electron microscopy (TEM) *etc.* Phenomenal progress in the field of ultra high pressures

has been made during recent years due to the development of the diamond anvil cell (DAC) and Raman studies upto 40 GPa are routinely possible in samples of interest to physicist

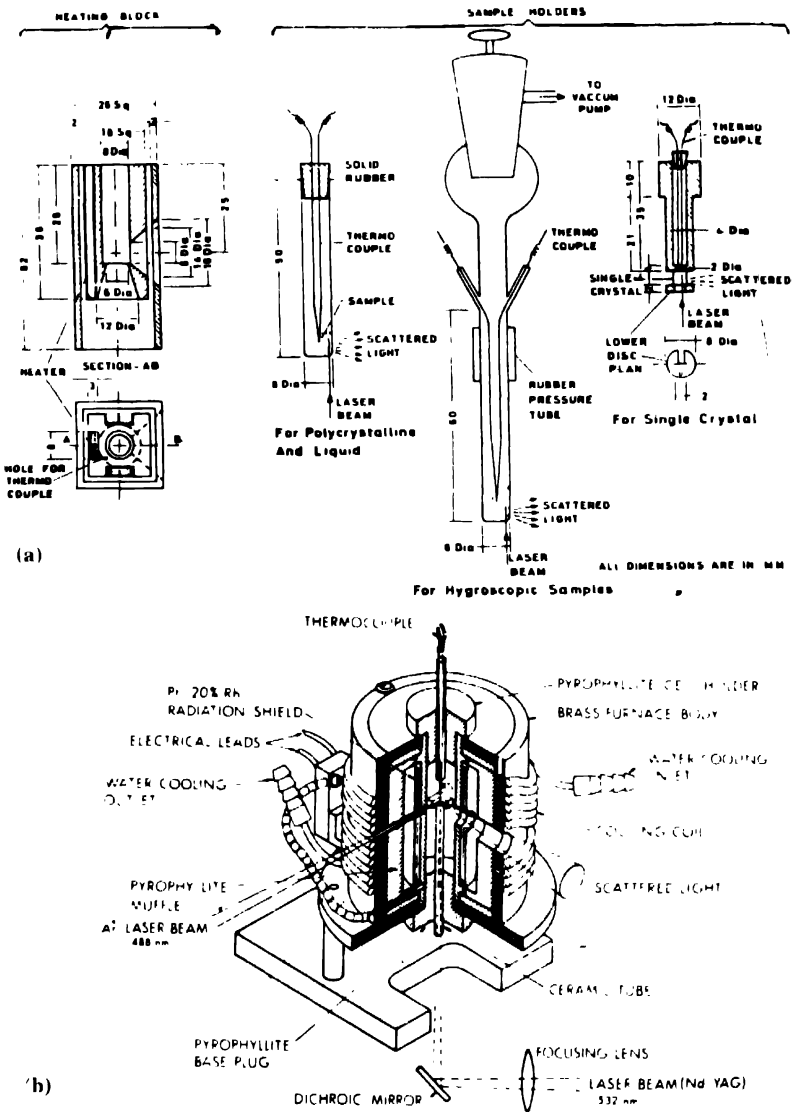

Figure 5. Design of high temperature cells for Raman (and PL) studies (a) different types of sample holders for upto 600° K, (b) a windowless Pt-10% Rh wire wound furnace upto 1400° K (after Sharma [17])

(lattice dynamics *etc*), chemists (materials), geophycists (minerals) and others. A few systems (solid H_2 and N_2) have been taken to megabar pressures [18,19] The diamond flat

typically of 300 microns diameter, with low photo-luminescence is essential for the DAC device along with fine focussing optics. As the sample could be less than 30 microns in the 300 micron flat; and, because of pressure gradients, the probing area is restricted to less than 5 micron diameter. Ar and Xe gases are used as pressure media for the samples. The small signals especially at high pressures need high sensitivity photon detectors. Most of the equipments are built around an optical microscope adopted to both for 180° and 145° scattering geometries with CCD or OMA detectors [17–21].

Organic molecular crystals undergo a large compression even at moderate pressures and exhibit large pressure shifts both in electronic and vibrational data [18]. Interesting studies on H_2, D_2 (upto 5 megabars), N_2 upto 1.6 M bar, diamond and zinc-blende materials, SiO_2-polymorphous and glasses has been published, recently [18,19].

4.7. Matrix isolation spectroscopy.

To obtain spectra of isolated or unstable (metastable) molecules, the technique of freezing them in inert gas/liquid matrices is used. The Raman spectra could be obtained by carefully preparing the matrix and avoiding fluorescence (due to diffusion pump oil or other impurities) [22]

4.8. Quenching and minimization of fluorescence background:

Since the quantum efficiency of PL is high as compared to RS, it is essential to minimize the fluorescence from the scattering volume. In many cases, where the fluorescence is due to impurities, purification of the sample is usually the most satisfactory method for reducing fluorescence background. Secondly, the sample can be positioned in front of the collection optics and irradiated (with the slits closed) with high incident laser power for a prolonged time. This bleaching of the impurities for colourless samples is most effective when the sample is stationary. Quenching agents such as potassium iodide (in solutions) [23] or mercury halides (vapor phase) may be added [24]. A mode-lock laser may be employed, and single photon-counting techniques may be used to achieve time discrimination in the picosecond range. Repetitive scanning and background subtraction may be employed. The initial two suggestions are not applicable if the sample itself is fluorescent. In that event switching to longer exciting wavelength should be tried before using external impurities like alkali or alkaline halide vapours. The Fourier transform (long wavelength excitation) Raman spectroscopy could be used. Alternatively, the sample may be cooled, to sharpen the energy levels and avoid absorption.

5. Raman instruments

We developed two modern state-of-the-art (at the time of installation ≈1980 and ≈1990 onwards) facilities for Raman studies at IIT, Kanpur.

5.1. The 1403 Ramalog system:

A block diagram for laser Raman work, using Spex 1403 Ramalog machine under Indian experimental conditions (which should be applicable to most southern tropical developing

countries) is given in Figure 6. The voltage stabilizer is essential to eliminate the voltage fluctuations if the input voltage varies within 150–250 V. The three phase stabilizers give

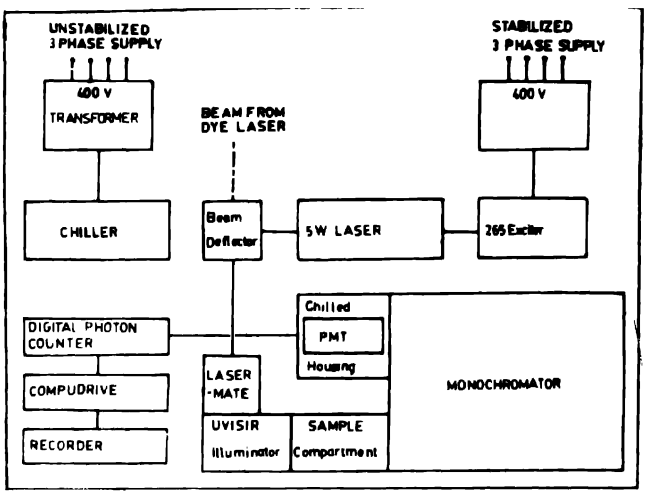

Figure 6. Block diagram for normal laser Raman (Ramalog) set-up at the Indian Institute of Technology (I I T), Kanpur

phase to phase constant voltage of 400 ± 5 V for 5 Watt Spectra Physics Ar^+ laser. The water cooled Neslab HX-500 recirculating heat exchanger (chiller plant), run on transformed 3 phase, 115 volts is used to cool the 5W laser head and Spectra Physics 265 exciter. The chiller is essential as the tap water, which is pumped directly from underground wells at the Indian Institute of Technology (IIT), Kanpur, maintains a temperature of almost 31°C throughout the year.

5.2. The optical system for Ramalog machine :

An optical line diagram is shown in Figure 7 for the Ramalog machine. The output beam from the laser is directed through a beam deflector M to the 'laser-mate', (a small grating spectrometer, used to get rid of the background plasma lines from the laser). The 'UVISIR illuminator' is the sample compartment. The laser line, free from plasma background, falls on the sample. The scattered light from the sample is collected through a combination of an elliptical mirror and plane mirror onto the first entrance slit S_1 of a double monochromator The scattered radiations are seen at 90° geometry after dispersion through the 1403 Ramalog machine by a C-31034/76 Ga-As photomultiplier (PMT) housed in a chamber thermoelectrically chilled to –30°C through Peltier cooling to reduce the dark counts (≈ 30 per second).

5.3. The Spex-1877D triplemate :

For micro Raman set up using Spex-1877D Triplemate under Indian experimental conditions (which should be applicable to most of the tropical developing countries), a block

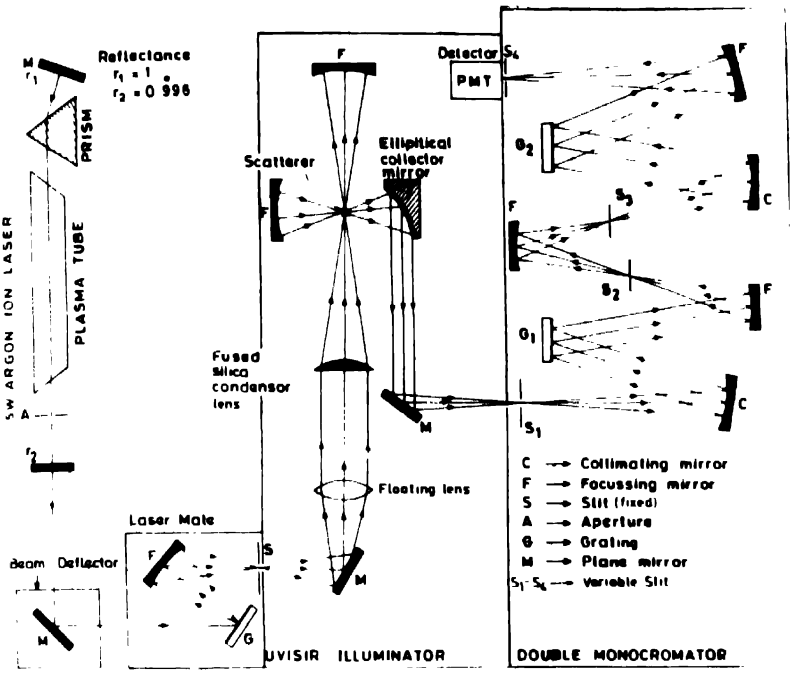

Figure 7. Ray-diagram of Spectra Physics Laser and Ramalog 1403 spectrometer at I I T, Kanpur

diagram is given in Figure 8. A saturated core automatic servo upconvertor and stabilizer gives a constant voltage output of 280 V ± 3 V per phase, even when any of its input phases varies between 150 to 250 V. The phase-to-phase voltage is stabilized at 480 volts. Likewise the three phase voltage stabilizer, shown on right hand top side, is essential to eliminate the voltage fluctuations for operating the delicate electronics used for driving the triplemate The input supplies for the multi-scan drive (MSD), photomultiplier tube (PMT), charge coupled device (CCD), interface unit, personal computer, printer, video camera (VC), and its monitor; all the components are operated through this stabilized power supply (230 V) after down conversion where essential. Two air-cooled (CA) HX-750 units from Neslab, having a total chilling capability of 48 KW (filled with conductivity water in their 150 litre tanks) are run on 3 phase, 230 volts and are used to absorb about 38 KW heat generated by 20 W Ar^+ Spectra Physics laser head, the dye laser and their power supplies. The chillers are essential, as mentioned earlier since the tap water which is pumped directly from underground water-wells at the Indian Institute of Technology, Kanpur, maintains a temperature of about 31°C throughout the year.

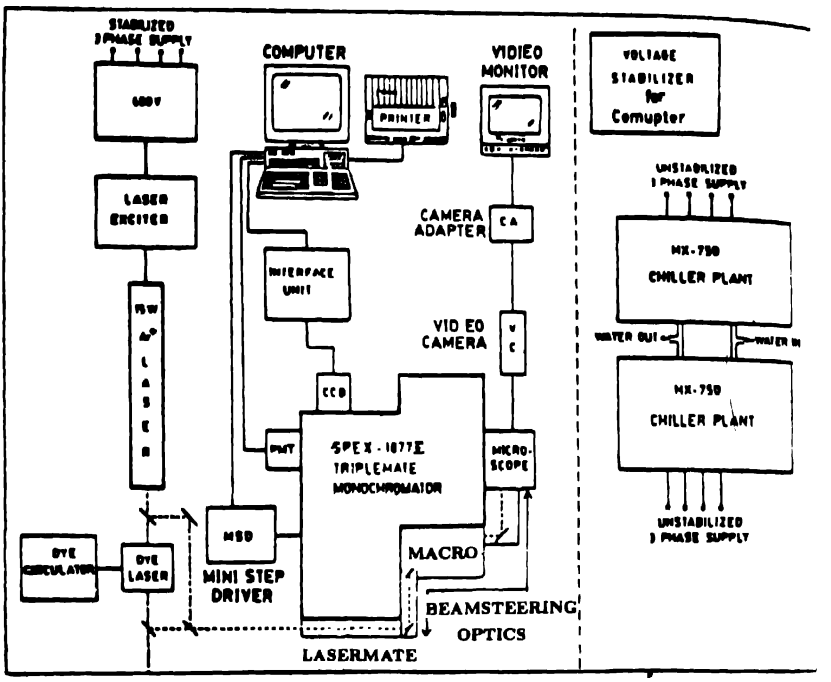

Figure 8. A schematic diagram of Micro Raman (with PMT and CCD) detector spectrometer system at I I T , Kanpur

5.4. The optical system for triplemate micro Raman system .

The optical ray diagram of the micro-Raman system is given in Figure 9. Normally about 1 W of output monochromatic line (usually 514.5 nm) from 20 W multiline Ar^+ laser is incident through the directing, and collimating, mirrors onto the grating G. The slit S removes the plasma lines. The lens L, five other mirrors and collimating lens, ordinary and dense filters, direct the incident beam to the sample (objective) stage of the microscope through the beam splitter. The back scattered light through the same microscope objective is directed through the same beam splitter and three lens combinations onto the entrance slit S_1 of the triplemate. The triplemate consists of a filter and a spectrograph stage. The filter stage has two modified Czerny-Turner spectrometers coupled in a substractive mode, each having a 50 × 50 mm plane grating (600 lines/mm) and having a band pass of about 1100 cm^{-1} on using 5 mm wide intermediate slit. In the spectrograph stage an asymmetric Czerny-Turner mount with a 64 × 64 mm^2 plane grating with 1200 lines/mm, is used to produce a dispersion of 1.4 nm/mm.

Inside the triplemate the light passing through S_1 is collimated by a mirror C onto G_1 and therefrom it is dispersed onto focussing mirror F. After passing through S_2, which determines the band pass of the filter stage, the light strikes the spatial filter (SF) mirror

and passes through the fixed slit S_3, which eliminates the stray light. Subsequently the light is collimated and dispersed, in an opposite direction to cancel the effects of the initial dispersion. Finally, it is focussed onto the exit slit of the filter stage (S_4), to control the resolution of 0.6 meter single spectrograph stage. The final collimation, dispersion and camera focussing-mirrors project a flat image onto the focal plane of the CCD (or PMT slit S_5).

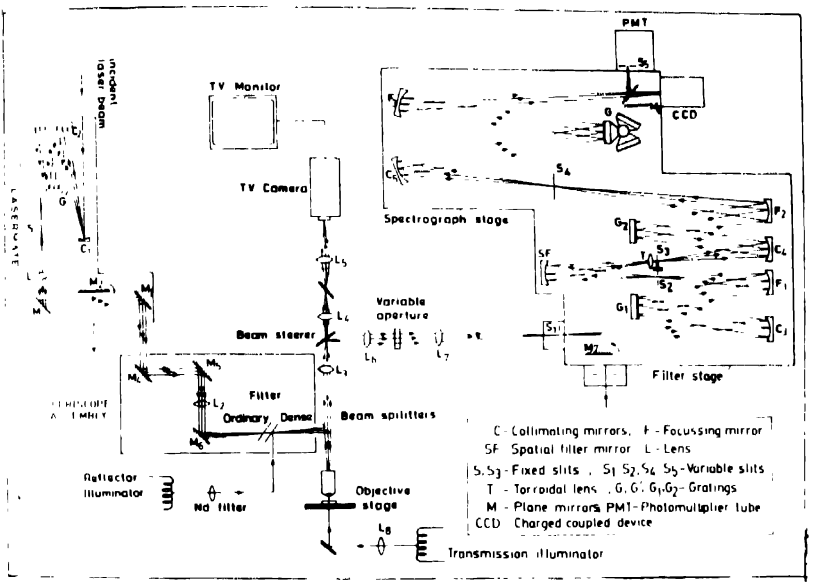

Figure 9. Optical diagram of Micro-Raman spectrometer at I I T, Kanpur

A flat, undistorted focal plane is essential for sensitive work with optical multichannel detectors (like videocons, diode-arrays or charge coupled devices). This is achieved by vignetting the field with the help of a torridal lens (T) which flattens the response of the non-dispersed segment of the band pass received from the exit slit of the filter double monochromator (0.22 meter), equipped with gratings locked in a subtractive dispersion mode. The spectral coverage of the CCD is limited to ≈ 650 cm^{-1} due to its 12.5 mm length, although a focal plane of 25 × 10 mm (high) could be obtained in this system. The spectra are reproducible to within ± 2 cm^{-1} with a resolution of 2 cm^{-1} for a particular scan setting of the spectrometer. The Si (521 cm^{-1}) or diamond (1332 cm^{-1}) are used for calibrating the observed data.

5.5 *Liquid nitrogen cooled charge coupled detector (LNC-CCD)*

The LNC-CCD from Astromed is an integrated charge coupled device which contains discrete 2D arrays (with an area of 8.5 × 12.5 mm^2) of 385 × 578 pixels. The potential wells are capable of trapping electrons and can be moved around, one at a time within the

semiconductor, by applying a varying potential to the electrodes on the surface of the device. The output amplifies measures charge in each of the potential wells and produces the output signal covering a range about 650 cm^{-1} in the system with grating G having 1200 lines/mm.

The LNC-CCD operates at 140 K. The dark current resulting from charges through thermal excitation (minimizing the charges produced by incident photons) is reduced at 140 K with respect to room temperature and longer integration times are possible without degradation of data during read out of images. The efficiency of the CCD is almost similar to that of a photomultiplier tube to detect ultra low light levels, but averaging capacity is like that of a photographic plate. The extended spectral range (200 to 1200 nm) becomes possible in this UV sensitized CCD— which provides a dynamic range of 10^5 with full imaging capability. The laser line with 500 mW at 752 nm would be most effective to make use of its maximum sensitivity. A correlated double (differential) sampling technique could be used to minimize the differential noise sources associated with the charge sensing process.

6. Raman spectroscopy applications

The micro-Raman technique is being used for tackling problems in geochemistry and geophysics (for study of rocks, ores and minerals) especially for solid and fluid inclusions [18,19]. Likewise identification, localization and characterization of gems, art materials, ancient sculptures, manuscripts and paintings, dust pollutants (sulphates, silicates, oxides, particles); impurities in normal, bio-organic and inorganic materials (papers, textiles, plastics, ceramics, semiconducts, food, drugs, product of metabolism *etc*); evolution of molecular or crystalline composition and distribution of species in microscopic samples during chemical reactions (corrosion, thermal degradation, photochemical processes, electrochemistry, catalysis *etc*) have been achieved by this novel technique [18–25]. We have established this facility at IIT, Kanpur, in 1990.

The optical levitation technique (in which 10 to 30 μm, microsized solid particles are trapped in stable optical potential wells of the focussed beam of radiation from a cw laser) has been used to study Mie's natural mode resonances in Raman spectra of small glass spheres [26].

With dye lasers, the wavelength of excitation, λ_{ex}, could be matched with electronic absorption bands of any sample to get the condition of resonance Raman scattering. One could get 3 to 4 orders of magnitude resonance enhancement with lower input excitation intensities on biological, biomedical and other delicate samples to study their ground and electronically excited states. The low lying electronic states of the same parity as the ground state (*e.g.* in Eu^{3+}, GaP, Zn, Mg which have very low scattering cross section σ_{Ram}) have been investigated by this technique [27,28].

The surface enhanced Raman spectroscopy (SERS) also enhances Raman scattering cross section, σ_{Ram}, by 10^2 to 10^6 for molecules inside absorbates and microscopic structures of surfaces and interfaces due to 'long-range electromagnetic' or a short range 'chemical communication' between the absorbate and the substrate. SERS produces vibrational signatures without external perturbations (as in infra red method) with good resolution (unlike LEEDS) [29].

The laser fields at two different frequencies, ν_L and ν_S can force a Raman mode ν_R for a medium to produce an oscillating dielectric constant, which interacts with the laser fields to produce directed coherent output beam frequencies $n\nu_L \pm m\nu_S$ with intensity comparable with the parent laser(s) [30].

7. Controlled micro-oxidation on the surface of Cd-Te single crystals [39]

Single crystals of CdTe are used for fabrication of high efficiency solar cell structures, nuclear radiation detectors, electro-optic modulators, laser windows, substrate material for HgCdTe based opto-electronic devices and in the epitaxy of other II-VI compounds for electronic and electro-luminescent applications. CdTe has been shown to exhibit infrared photorefractivity and has acquired additional significance recently [40,41].

Insulating oxides from specific semiconductors are essential for the development of electronic and opto-electronic devices [42,43]. Amorphous oxygenated CdTe (a-CdTe : O) films have been grown by the *r.f.* sputtering deposition technique in an Ar–N–O atmosphere [44,45] and a ternay amorphous compounds ($CdTe_{1-x}O_x$, where the band gap of CdTe changes between 1.48 to 3.35 eV and the resistivity changes from 10^4 to 10^{12} Ω cm on controlled oxygenation[2] has been suggested [44].

We provide an example of monitoring a controlled surface oxidation on a micro-(nano-) meter scale in single crystals or wafers of CdTe using controlled laser irradiation under ambient conditions with N_2 serving as a catalyst and O_2 providing necessary oxidation. This process may provide interesting example of nanostructures of CdTe/Cd-Te-O system with dispersion of semiconductor (CdTe) nanostructures in an insulator Cd-Te-O system or *vice-versa*. The semiconductor nanocrystals dispersed in transparent matrices are known to present highly enhanced optical nonlinearities and relaxation effects due to the zero-dimensional quantum confinement of phonons as well as electron-hole pairs. The nonlinear properties of these hetero-phase systems with nanocrystal aggregates are strongly affected by the average size and size-distribution of nanocrystals. To study the species formed, the fundamental vibrational region would be most appropriate. Additionally, the CdTe oxide passivation may be tremendously helpful for optoelectronic device fabrication similar to the role of SiO_2 in the Si-technology [43,44].

The controlled oxidation of CdTe and its *in-situ* monitoring using Raman spectroscopy in the 50–1250 cm^{-1} range is presented.

7.1. Growth of single crystals and their characterization and recording of spectra:

Crystals of CdTe were grown using the travelling heater method (THM) [45] using 99.999% (metal basis) pure tellurium, and 99.9999% pure Cd. The tellurium was further zone refined using a laboratory built apparatus having two source heaters. A typical charge of 75 g tellurium was loaded into a clean and outgassed quartz ampoule, evacuated and sealed. Zone refining was performed for a total of 45 passes at 1.5 cm/h. The central part of the zone refined ingots were mixed with the other starting elements and loaded into 15 cm long quartz ampoules, evacuated and sealed. The synthesis reaction was performed in a laboratory built rocking furnace kept at 800°C for one week. A three zone vertical furnace was employed to grow the crystals from the melt near the melting temperature (approx. 1100) using a heater translation rate of 0.1 cm/h. Large grain single crystal ingots having 1 cm diameter and about 6 cm long were obtained.

Raman measurements have been made using ≈180° backscattering geometry. In this recording configuration the wavevector of the scattered photon (q_s), is approximately anti-parallel to the excitation photon-wavevector (q_i). Hence, the wavevector of the interacting scattered phonon q should be $2q_i$, which is negligibly small compared to zone boundary wavevector, and hence zero wavevector phonons are expected. Low signal to-noise ratio in CCD (140°K) was achieved for accumulation times of upto 15 minutes for each spectrum leaving the same amount of time for background to be subtracted, and allowing heat relaxation during this period. Each accumulated spectrum was smoothened (whenever necessary) with a Fourier filtering algorithm using the peak fit program (Jandel Scientific Software). The Lorentzian fitting for various sample lines [46] has been applied to obtain the total integrated intensities.

7.2. Controlled evolution of TeO_3^{2-} on the surface of CdTe

Excess Te appears on the surface of single crystals of CdTe. The formation of an oxide of Te on sample standing in air for long time is expected.

Figure 10 shows the relevant portions of the spectra obtained in the 50–850 cm^{-1} regions from about < 2 μm diameter spot of the sample of CdTe single crystals with a 2 mW Ar^+ laser beam falling on (a) virgin spot and (b) a spot after irradiating with 13.5 mW power of the same laser for about 15 minutes. The Raman bands observed in the spectra are given in Table 3, along with the most probable assignments. The unambiguous detection of $[TeO_3]^{2-}$ radical is established.

7.3. The tellurium modes:

Te aggregates of diameters of several nanometers could easily be prepared by using dilute acids (15% solution of concentrated HNO_3) for approximately two minutes on the surface of freshly cleaved tellurium [47]. The tellurium modes near 92, 103, 123 and 141 (partially) could be assigned to the presence of Te on the surface of CdTe [47]. Te has at least two orders of magnitude larger scattering cross section compared to that of CdTe.

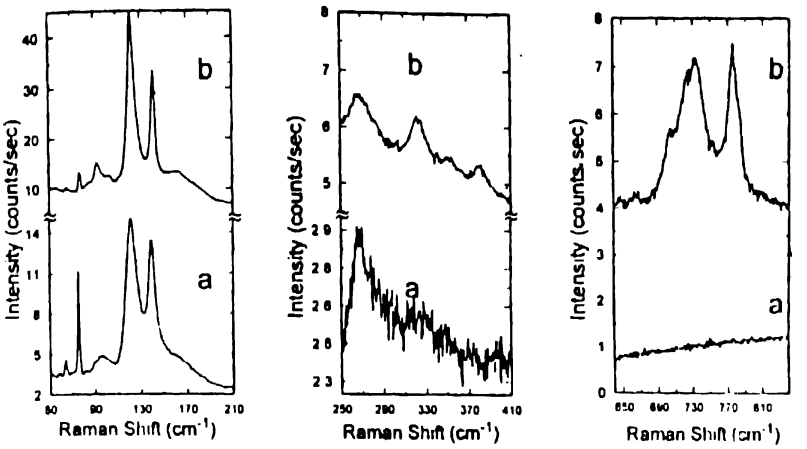

Figure 10. Relevant portions of the micro-Raman spectra excited by 514.5 nm (2 mW) laser from a sample of CdTe having a spot diameter of <2 μm (a) virgin spot and (b) spot irradiated with 13.5 mW power for about 15 minutes

Our samples retained the Te bands. This is consistent with the view that bulk CdTe crystals, grown by different techniques contain Te precipitates due to the retrograde shape of the solids near the melting point.

Table 3. Observed Raman transitions (cm^{-1}) in CdTe in dilute solution [50], and in single crystal both in virgin and irradiated spots at room temperature (a), (b) and (c) are after references [47], [48] and [50]. The words w, v, s, m, sh and b within parentheses have been used to denote the nature of bands: weak, very, strong, medium, shoulder and broad, in that order.

Virgin spot	Irradiated spot	Assignments
96.9 (w)	92 (w)	$\nu_{Te}(E)^{(a)}$
	103 (vw)	$\nu_{Te}^{(a)}$
123 (V)	123 (vs)	$\nu_{Te}(A_1)^{(a)}$
141 (m)	141 (m)	TO (CdTe)$^{(b)}$ + $\nu_{Te(L)}^{(a)}$
167 (sh)	167 (sh)	LO (CdTe) (b)
	174 (vw)	2 × 92 (Te)
269 (vw, b)	269 (vw, b)	2 × 141 (2TO)
	324 (vw) 326$^{(c)}$	$\nu_4^{(L)}(TeO_3^{2-})$
	364 (m), 364$^{(c)}$	$\nu_2(A_1)(TeO_3^{2-})$
	381 w (vvw)	$\nu_4(E)(TeO_3^{2-})$
	662 (vvw)	$\nu_3(E)(TeO_3^{2-})$
	703 (vvw), 703$^{(c)}$	$\nu_3(E)(TeO_3^{2-})$
	732 (vs), 758$^{(c)}$	$\nu_1(TeO_3^{2-})$
	775 (m)	$2\nu_4(E)(TeO_3^{2-})$

7.4. The CdTe bands :

The single crystals of CdTe exhibit longitudinal optical LO phonons (≈167 cm^{-1}) along <100> and <111> faces and TO phonons (141 cm^{-1}) along <110> and <111> planes [48]. In our sample the laser was incident over <111> surface, which implies that both LO and TO phonons should be present in the observed spectra. The proper assignments [48] of the CdTe phonons is also given in Table 3 both for the virgin and irradiated spots. The two phonon band at 269 cm^{-1} is attributed to the anharmonic effects in the system. The anharmonic coefficient [2TO (calc.)–2TO (observed)] of 13 cm^{-1} is quite reasonable. The larger half width of this band is also consistent with its assignment as a two phonon band.

7.5. TeO_3^{2-} optical phonons :

The isolated symmetric bent TeO_3^{2-} ion belongs to the pyramidal structure belonging to the C_{3v} point group. For this point group all of the four normal modes of vibration are Raman (and infrared) active. The observed normal modes of the ion in dilute solutions are given in Table 3 along with the symmetry species, A_1 and E [50]. The totally symmetric Te–O stretching mode ν_1 at 758 cm^{-1} is higher than the doubly degenerate asymmetric stretching mode ν_3 at 703 cm^{-1}. Likewise, the symmetric deformation mode ν_2 at 364 cm^{-1} is higher than the asymmetric doubly degenerate deformation mode ν_4 at 326 cm^{-1} [50,51]. On lowering the symmetry to C_{2v} or C_s the doubly degenerate modes would exhibit splitting Likewise, in crystalline environment, shifting of these modes under crystal potential and site symmetry or factor-group splittings are expected. Hence the total number of observed bands could be six (all active in Raman and infrared under C_s symmetry) or any higher number depending upon the crystalline field, the number of atoms per primitive cell *etc* Additionally the surface nano- (micro-) structures would exhibit quantum dot (zero-dimensional), quantum rod (one-dimensional), quantum surface (two-dimensional) or quantum size (3-dimensional) effects. The tellurate is produced within 2 μm diameter with free Te aggregate and CdTe lattice around it are likely to exhibit several of the above effects. Thus, the evidence of nano-structures within micron sized spot is illustrated through micro-Raman spectroscopy.

For a comparison, the extra bands observed from irradiated spot in Figure 10, are also given in Table 3 along with their assignments. The following conclusions are drawn : (a) the degenerate deformation mode ν_4, falling in the free TeO_3^{2-} at 326 cm^{-1} shows lifting of degeneracy with components at 324 and 381 cm^{-1}. Likewise, the degenerate asymmetric stretching mode ν_3 (E) falling at 703 cm^{-1} exhibits weaker two components at 662 and 703 cm^{-1}. There seems a remarkable coincidence of the $\nu_2(A_1)$ mode (falling exactly at 364 cm^{-1} in the CdTe-Te-TeO_3^{2-} environment) to the free TeO_3^{2-} ion band at 364 cm^{-1} in solutions. The totally symmetric mode $\nu_1(A_1)$ in the TeO_3^{2-} exhibits a Fermi-resonance with the unshifted position at 746.5 cm^{-1} showing a small shift (11.5 cm^{-1}) to lower frequency side as compared to the free ion position at 758 cm^{-1}.

7 6. Fermi resonance in TeO_3^{2-} bands :

Whenever two vibrational levels belonging to different vibrations (or combinations of vibrations) having nearly the same energy, and symmetry species, fall near each other, only the perturbed levels are observed in the spectrum [52,53]. The unperturbed separations δ between the two positions could be calculated by using the simple relation between the observed intensities I_1 and I_2 of the two bands and the observed (perturbed) separation Δ of the bands [52] by the simple expression $I_1/I_2 = (\Delta + \delta)/(\Delta - \delta)$. In the recorded spectrum in the 720–800 cm^{-1} region two prominent peaks have been observed at 732 and 777 cm^{-1} with total separation of 45 cm^{-1}, and total area enclosed by them is in the ratio 2.009 to 1 arbitrary units. Using the above expression, the unperturbed separation δ is calculated as 15.9 cm^{-1}. The final position of the totally symmetric ν_1 band of TeO_3^{2-} in solution and in the present case before and after perturbation is depicted in Figure 11 by the continuous line. The perturbing level is evidently the overtone of the splitted component of the asymmetric bending mode, ν_4, falling at 381 cm^{-1}. The ν_1 mode in theTeO_3^{2-} system would have been in position ii(a) at 746.5 cm^{-1}. However due to the Fermi resonance it is displaced further to position ii(b) at 732 cm^{-1}. The mean position of Fermi-pair 732–777 cm^{-1} is 754.5 cm^{-1} and it is very close to the position of this band in dilute solution at 758 cm^{-1}. Small shift of the Fermi doublet on higher irradiation power (Table 4) has also been observed.

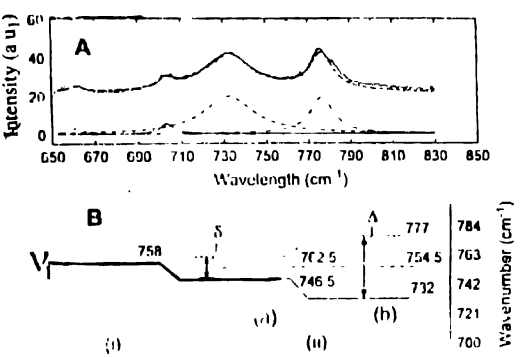

Figure 11. The main bands 732 and 777 cm^{-1} in the Raman spectrum of TeO_3^{2-} on CdTe [A] observed spectrum and Lorentzian peak fit analysis in the 650–830 cm^{-1} range [B] ν_1 band (—) in (i) dilute solution and (ii) unperturbed calculated positions (a), and perturbed (due to Fermi Resonance) positions (b) of ν_1 band (—) and $2\nu_4$ band (----), on the surface of CdTe–Te–TeO_3^{2-}. The 754.5 cm^{-1} (- - -) represents the mean of the two band positions

7 7. The photoluminescence of CdTe :

We have made an extensive study of the photoluminescence (PL) of CdTe samples.Six excitation wavelengths namely, 514.5, 501.7, 496.5, 488.0, 476.5 and 457.9 nm were used. The temperature dependence of the PL was also studied. Relevant portions of a typical PL

spectrum of CdTe crystal observed on excitation with ≈2 mW of 457.9 nm laser light on the sample at ≈25 K are given in Figure 12. A sharp peak at 1.60 eV which is unambiguously assigned to the emission maximum of near-band-gap transition of CdTe. The band-gap at 5 K is 1.61 eV [54]. The broader shoulder at 1.48 eV and the most intense peak at 1.45 eV in the PL spectrum have been associated with defects due to Cd and Te respectively [54].

Table 4. The observed bands in 650–830 cm^{-1} due to Fermi Resonance of ν_1 and $2\nu'_4$ bands of TeO_3^{2-} ion with 2 mW and 13.5 mW excitation powers

Band position cm^{-1} with excitation powers	
2 mW	13.5 mW
732 (14)*	727 (18.4)
777 (6, 7)	763 (10.9)

*The values in parenthesis denote FWHM in cm^{-1}

This study suggests the detection of CdTe from the sample on the basis of more sensitive PL studies. It has been observed that TeO_3^{2-} ion production results in the diminution of the overall PL signals due to CdTe crystals.

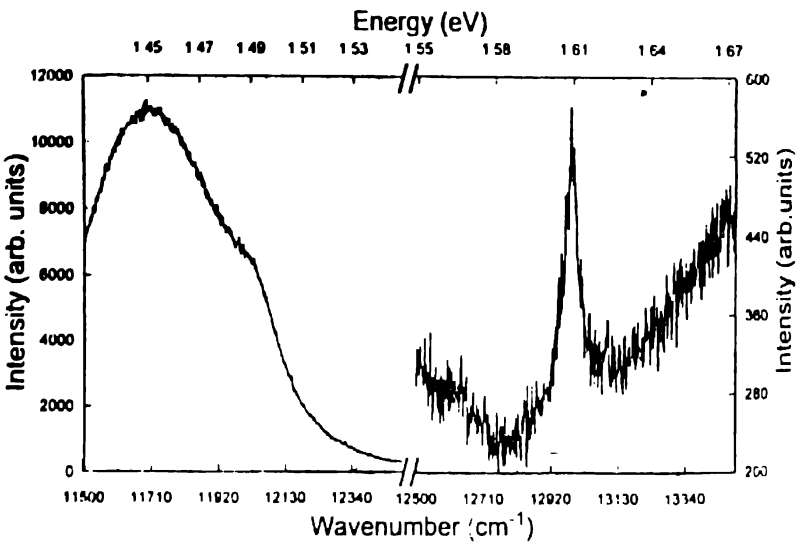

Figure 12. Photoluminescence spectrum of CdTe at ≈25 K with 457 9 nm laser excitation

Conclusions

On the basis of a combined micro Raman and photoluminescence studies the simultaneous existence of CdTe and Te aggregates distributed over the surface (and entire

volume) of the crystal is suggested. On irradiation with an intense laser power TeO_3^{2-} ions are created within <2 μm diameter spot on the surface of CdTe crystal. The study is important to explore the mutual interactions of the Te aggregates, TeO_3^{2-} ion and CdTe semiconductor.

8. Inhomogeneity within GaAs/$Al_xGa_{1-x}As$ oval defects

(a) Crystalline orientation : 100(LO), 110(TO), 111(LO, TO) :

Micro-Raman studies have been carried out to investigate the crystalline inhomogeneities in the periphery and inside the oval defects sized ≈2 to 20 μm in GaAs and $Al_x Ga_{1-x}$ As epitaxial layers. Figures 13(a), (b), (c) and (d) display spectra taken from different points of 2×10^{16}, 2×10^{17}, 5×10^{17} and 3×10^{18} cm^{-3}, Si-doped GaAs in that order. A sharp LO phonon lines at 292 ± 1 cm^{-1} from normal regions indicates the perfect orientation of epilayers as (100) plane. In the 3×10^{18} cm^{-3} the position of TO mode is taken by the *L* mode. In the spectra under the oval defects, the additional appearance of TO modes at 269 ± 1 cm^{-1} is interpreted as an important deviation of crystalline orientation [55]. As the (111) propagating phonon allows both LO and TO modes in backscattering geometry, the comparable intensity of LO-TO modes in Figure 13(a) indicates the (111) plane at the center of the oval defects [56]. As the Si-dodping increases in Figure 13(b) and 13(d), the TO mode gains intensity very rapidly while the LO mode intensity drops systematically.

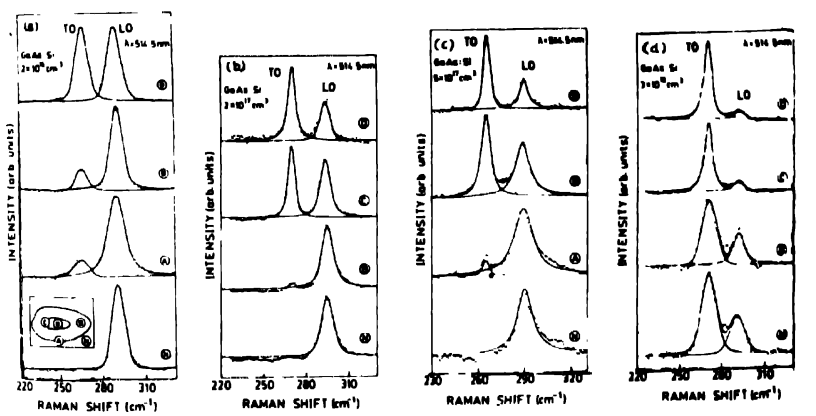

Figure 13. Depolarized room temperature Raman spectra taken from the various spots in and around the oval defect in (a) 2×10^{16}, (b) 2×10^{17}, (c) 5×10^{17} and (d) 3×10^{18} cm^{-3} Si-doped GaAs. The inset shows the trace of a typical oval defect. The various spots A, B, C and D are the defect spots and N is from defect-free regions. The circles around these spots show the approximate size of the focussed laser beam

These observations suggest that the crystalline morphology at the center of oval defects becomes more (110) type with increasing Si-doping in GaAs [57].

Similar variation of crystalline orientation was also observed in $Al_x Ga_{1-x} As$ oval defects. In addition, tensile and compressive stresses have been inferred in the oval defects of direct ($0 < x < 0.4$) and indirect ($0.4 < x < 1$) gap $Al_x Ga_{1-x}$. As alloys.

(b) Carrier concentration :

In polar semiconductors a strong coupling between the LO phonons and the free carriers exists if the plasma frequency is comparable to the LO phonon frequency. Because of this coupling the plasmons and phonons cease to be independent excitations and two mixed plasmon-LO phonon modes labelled L^+ and L^- are observed. The frequencies of these two coupled modes follow [58].

$$\omega_{\pm}^2 = \frac{1}{2}\left\{\left(\omega_p^2 + \omega_{LO}^2\right) \pm \left[\left(\omega_p^2 + \omega_{LO}^2\right)^2 - 4\omega_p^2\omega_{TO}^2\right]^{1/2}\right. \quad (1)$$

This variaton of the frequencies of $L\pm$ modes with carrier concentration is shown in Figure 14.

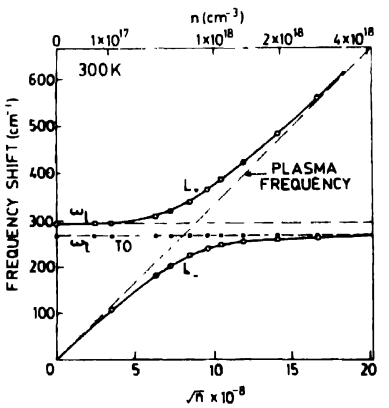

Figure 14. Frequency shift of Raman scattered $L\pm$ phonon-plasmon mixed modes with carrier density (n cm^{-3}) in GaAs at room temperature

Various oval defects and normal regions were excited in Si-doped GaAs samples The experimentally observed values of peak frequencies of $L\pm$ modes have been utilized to deduce the carrier concentrations (n_e) at various spots through the relation $\omega_p = (4\pi n_e^2 / m^* \varepsilon_\infty)^{1/2}$. Where ε_∞ is the high frequency dielectric constant and m^* is the effective mass of the carriers.

The obtained carrier concentration at normal regions and defect spots in 5×10^{17} and 3×10^{18} cm^{-3} Si-doped GaAs samples have been presented [59].

As an alternate method, the variation of surface depletion width with normal region carrier concentration have been used to find the concentration at the oval defects [59]. The observed intensities of LO and TO modes from various excitation spots are discussed. Using these intensities the depletion width Ls was calculated at the oval defects.

From the calculated value of Ls the carrier concentration at the oval defects was deduced using the carrier density variation with depletion width at defect free regions. The carrier concentration obtained from intensity ratio (depletion width) is computed and was found very close to that deduced from the position of $L\pm$ modes. It has been demonstrated that the carrier density at the various oval defects of GaAs is lower than that in the respective epitaxial layers [59].

Acknowledgment

Thanks are due to Council of Scientific and Industrial Research specially for award of Emeritus Scientistship, Department of Science and Technology and the Ministry of Human Resource Development for generous funding on several projects. Thanks are also due to Professor J Narayan, Professor J R Durig, Professor A Aslam and Professor R S Kattyar for making the samples and facilities available for collaborative work.

References

[1] H D Bist and S Bhargava *Laser and their Applications, the Indian Spectrum for 2001 AD* (New Delhi Tata McGraw Hill) (1996)

[2] H D Bist, R K Thareja, A Pradhan and P K Khulbe *Advanced Laser Spectroscopy and Applications* (New Delhi Allied Publishers) (1996)

[3] H D Bist, J R Durig and J F Sullivan *Raman Spectroscopy Sixty Years On* **Vol I** (Amsterdam Elsevier) (1990)

[4] H D Bist, J R Durig and J F Sullivan *Raman Spectroscopy Sixty Year On* **Vol II** (Amsterdam Elsevier) (1990)

[5] H D Bist, D P Khandelwal and G Chakrapani *Lasers and Applications in the Indian Context* (New Delhi Tata McGraw Hill) (1985)

[6] H D Bist and J S Goela *Lasers and Applications* (New Delhi Tata McGraw Hill) (1984)

[7] H D Bist *Laser Raman Spectroscopy and its Applications especially in Structural Phase Transitions Proc Indian Acad Sci (Chem Sci)* **103** 295 (1991)

[8] A Weber *in the Raman Effect* ed. A Anderson, (New York Marcel Dekker) (1973)

[9] H L Welsh and M F Crawford *Phys. Rev* **72** 524 (1947)

[10] H L Welsh, M F Crawford, T R Thomas and G R Love *Can J Phys* **30** 577 (1952)

[11] H D Bist and J C D Brand *J. Mol Spectrosc* **62** 60 (1976)

[12] H J Bernstein (Private Communication) (1976)

[13] W Kiefer and H J Bernstein *Applied Spectrosc* **25** 500 (1971)

[14] P S Dobal, H D Bist, G Morell, A Reynes-Figuroa, A Manivanam, R S Kattyar, S K Mehta and R K Jain *J Mater Sci* (1971)

[15] F A Miller and B M Harney *Appl Spectrosc* **C24** 291 (1970)

[16] D P Strommen and K Nakamoto *Laboratory Raman Spectroscopy* (New York · John Wiley & Sons) (1984)

[17] S K Sharma in *Raman Spectroscopy, Sixty years on* ed H D Bist, J R Durig and J F Sullivan **17B** pp 513 (1989)

[18] A Jayaraman in *Raman Spectroscopy, Sixty years on* ed. H D Bist, J R Durig and J F Sullivan (Amsterdam . Elsevier) (1989)

[19] A Jayaraman *Rev. Mod. Phys.* **58** 65 (1983)

[20] H K Mao, P M Bell and R J Hemley *Phys. Rev. Lett.* **55** 99 (1985)

[21] A Jayaraman, M L Kaplan and P H Schmidt *J Chem Phys.* **82** 1682 (1985)

[22] W Scheuermann and K Nakamoto *Appl. Spectrosc* **32** 251 (1978)

[23] J M Friedman and R M Hochstrasser *Chem. Phys Lett.* **33** 225 (1975)

[24] V A Maroni and P T Cunningham *Appl Spectrosc* **27** 428 (1973)

[25] M Bridoux, F Wallart and M Delhaye in *Lasers and Applications* eds H D Bist and J S Goela (New Delhi Tata McGraw-Hill) p 246 (1984)

[26] R Thurn and W Kiefer in *Lasers and Applications* eds H D Bist and J S Goela (New Delhi . Tata McGraw-Hill) p 234 (1984)

[27] B Hudson and J R Sension in *Raman Spectroscopy, Sixty Years On* eds H D Bist, J R Durig and J F Sullivan (Amsterdam Elsevier) **Vol I** p 363 (1989)

[28] K P Jain and R K Soni in *Raman Spectroscopy, Sixty Years On* eds H D Bist, J R Durig and J F Sullivan (Amsterdam Elsevier) **Vol I** p 262 (1989)

[29] R C Chang and T E Furtak eds *Surface Enhanced Ramana Scattering* (New York Plenum) (1982)

[30] N G Basov, A Z Grasiuk and I G Zubarev in *Raman Spectroscopy, Sixty Years On* eds H D Bist, J R Durig and J F Sullivan (Amsterdam · Elsevier) p 255 (1989)

[31] M V Klein in *Raman Spectroscopy, Sixty Years On* eds H D Bist, J R Durig and J F Sullivan (Amsterdam · Elsevier) p 203 (1989)

[32] A Pinczuk and J P Valladares in *Raman Spectroscopy, Sixty Years On* eds H D Bist, J R Durig and J F Sullivan (Amsterdam Elsevier) p 223 (1989)

[33] A Deffontaine in *Raman Spectroscopy, Sixty Years On* eds H D Bist, J R Durig and J F Sullivan (Amsterdam · Elsevier) p 323 (1989)

[34] S S Jha in *Raman Spectroscopy, Sixty Years On* eds H D Bist, J R Durig and J F Sullivan (Amsterdam Elsevier) p 337 (1989)

[35] R E Hester in *Raman Spectroscopy, Sixty Years On* eds. H D Bist, J R Durig and J F Sullivan (Amsterdam : Elsevier) p 351 (1989)

[36] P Hildebrandt and M Stockburger in *Raman Spectroscopy, Sixty Years On* eds H D Bist, J R Durig and J F Sullivan (Amsterdam . Elsevier) p 443 (1989)

[37] W L Peticolas in *Raman Spectroscopy, Sixty Years On* eds H D Bist, J R Durig and J F Sullivan (Amsterdam · Elsevier) p 467 (1989)

[38] A T Tu and S Zherg in *Raman Spectroscopy, Sixty Years On* eds H D Bist, J R Durig and J F Sullivan (Amsterdam . Elsevier) p 485 (1989)

[39] B K Rai, H D Bist, R S Katiyar, K T Chen and A Burger *J Appl. Phys.* **80(1)** 477 (1996)

[40] N V Sochinskii, M D Serrano, E Dieguez, F Agullo-Rueda, U Pal, J Piequeras and P Fernandez *J Appl Phys* **77** 2806 (1995)

[41] A Partovi, J Millerd, E M Garmire, M Ziari, W H Steier, S B Trivedi and M B Klein *Appl Phys Lett* **57** 846 (1990)

[42] E H Nicollian and J R Brews *in MOS (Metal Oxide Semiconductor) Physics and Technology* (New York John Wiley & Sons) p 4 (1982)

[43] D L Lile in *Gallium Arsenide Materials, Devices and Circuits* eds. M J Howes and D V Morgan (New York : John Wiley & Sons) pp 263 (1985)

[44] F J Espinoza Baltran, F Sanchez-Sinencio, O Zelaya-Angel, J G Mendoza-Alejo Armenta, C Vazquez-Lopez, M H Farias, G Soto, L Soto, L Cota-Araiza, J L Pena, J A Azamar Barrios and L Banos *Jpn. J. Appl. Phys.* **30** L1715 (1991)

[45] F J Espinoza-Beltran, O Zelaya, F Sanchez-Sinencio, J G Mendoza-Alvarez, M H Frias and L Banos *J Vac Sci. Tech.* **A11** 3062 (1993)

[46] G Morell, A Reynes-Figueroa, R S Katiyar, M H Farnah, F J Espinoza-Beltran, O Zelaya-Angel and F Sanchez-Sinencio *J Raman Spectrosc* **25** 203 (1994)

[47] R N Zitter *Surface Science* **28** 335 (1971)

[48] P M Amirtharaj and F H Pollak *Appl. Phys Lett* **45(7)** 789 (1984)

[49] Y Nishibayashi, Y Tokumitsu, T Imura and Y Osaka *Jpn J. Appl. Phys Part (1)* **28(10)** 1919 (1989)

[50] H Siebert Z *Anorg. Allg Chem.* **275** 225 (1955)

[51] K Nakamoto *Infrared and Raman Spectra of Inorganic and Coordination Compounds* (New York : John Wiley & Sons) pp 117 451 (1986)

[52] H D Bist, J C D Brand and D R Williams *J Mol Spectrosc* **21** 413 (1967)

[53] G Herzberg *Molecular Spectra & Molecular Structure II IR and Raman Spectra of Polyatomic Molecules* (New York : Van-Nostrand) pp 215 (1945)

[54] C B Davis, D D Allred, A Reyes-Mena, J Gonzalez Hernandez, O Gonzalez, B C Hess and W P Allred *Phys Rev.* **B47** 13363 (1993)

[55] G Burns, F H Dacol, C R Wie, E Burnstein and M Cardona *Solid State Commun.* **62** 449 (1987)

[56] P K Khulbe, P S Dobal, H D Bist, S K Mehta and R K Jain *Appl Phys Lett* **63** 488 (1993)

[57] P S Dobal, H D Bist, S K Mehta and R K Jain *Semicond Sci Technol* **11** 315 (1996)

[58] M V Klein in *Light Scattering in Solids I* ed M Cardona (Berlin : Springer) p 147 (1985)

[59] P S Dobal, H D Bist, S K Mehta and R K Jain *J. Appl Phys* **77** 3934 (1995)